Al-Fin BOND IN ALUMINUM PISTON ALLOY & AUSTENITIC CAST IRON INSERT

Srećko Manasijević, Radomir Radiša
LOLA Institute, Belgrade, Serbia

Zdenka Zovko Brodarac, Natalija Dolić
University of Zagreb, Sisak, Croatia

Mile Djurdjevic
Institute for Testing of Materials (IMS Institute), Belgrade, Serbia

Abstract

This paper presents the results of investigating an Al-Fin bond between an aluminum piston alloy and austenitic cast iron. The part investigated utilized an austenitic cast iron insert for the first ring groove for application in a highly loaded diesel engine for increased wear resistance. A metallographic investigation using an optical microscope in combination with SEM/EDS (Scanning Electron Microscopy/Energy Dispersive Spectroscopy) analysis and 3D visualization of the quality of the intermetallic bonding layer was performed. The test results show that a metallic bond can be formed between the aluminum piston alloy and the austenitic cast iron.

Keywords: *piston, piston alloy, Al-Fin bond, alfin, Ni-Resist, ring carrier, 3D visualization, austenitic cast iron, diesel engine applications*

INTRODUCTION

Pistons are made mostly of aluminum multicomponent alloys (Al–Si–Cu–Ni–Mg), which represent a special group of industrial alloys that are used in the automotive industry due to a good combination of casting and mechanical properties,[1] high strength at elevated temperatures (e.g. up to 350°C/662°F)[2] and resistance to sudden temperature change.[1–4]

Depending on the engine type and operating conditions, there are many different design solutions for pistons: mono metallic aluminum pistons, pistons with ring carrier, pistons with a cooling channel, pistons with a cooling channel and ring carrier, pistons with controlled expansion, pistons with controlled spreading and ring carrier, pistons with an iron coating, forged pistons, split pistons, pistons with the first groove reinforced, pistons with an undulating mantle, etc.[4]

In order to meet the requirements for lower fuel consumption, the mean effective pressure of diesel engines for commercial vehicles is growing. These are the engines that must be designed to withstand high loads for long periods of work, especially in the critical areas of pistons that are thermally highly-loaded. Today's aluminum pistons with a ring carrier can meet these requirements. The ring carrier is specially designed for the formation of the first piston ring groove in highly-loaded diesel engines. The ring carrier must have a very similar coefficient of thermal expansion with the aluminum piston alloy (1.93 x 10^{-6} K^{-1}).[4] The ring carriers are made of austenitic cast iron (Ni-Resist) in order to increase the wear-resistance of the first ring groove, especially in engines with high loads.[4–6] A wear-resisting piston ring carrier can reduce the temperature at the piston head, increase the resistance of the piston to wearing and dramatically increase the lifetime of the piston. It can also improve the air-tightness of the piston in the cylinder, increase the efficiency of combustion, and reduce emissions and air pollution.[4–10]

The ring carrier is produced using the centrifugal casting method. Manufacturers use many different shapes for the ring carrier to help lock it into the casting. The ring carrier is ring-shaped with different cross-sections. Most often, the outside diameter is 70–200mm (2.8–7.9 in.) while the inner diameter is 50–180mm (2.0–7.1 in.).[3] The real strength of the insert in the piston is the result of a molecular or atomic bond between the insert and the piston materials.[5–8] Producers also often use other improvements, such as a cooled ring carrier and the insertion of pin bore bushings, etc.

When a conventional casting (permanent mold casting) process is used to pour the liquid Al–Si alloy into the mold over the insert, the latter is simply embedded in the light alloy after solidification.[5–8] In effect, the iron and aluminum oxide layers prevent the establishment of a direct contact between the two metals and no real interfacial bond exists.[5–8] Using a special casting procedure derived from the "Al-Fin process" (alfin),[5–8] it has been possible to form an intermetallic bond at the insert/alloy interface. This approach has resulted in the design of lighter components with improved functionality.[5–8]

The alfin process is a method for preparing a ferrous surface for intermetallic bonding.[3–7] The alfin bonding process is commonly used to bond a nonferrous Al alloy and a ferrous alloy, such as aluminum diesel engine pistons and Ni-Resist ring carriers, directly together. It is well known that cast iron is a ferrous alloy that contains significantly higher levels of carbon and silicon than steel. During piston casting, the ring carrier is soaked by the alfin bond process, which results in a strong connection with the piston material. During this process, an intermetallic layer composed of Fe_xAl_y is formed on the border between the two different materials by the diffusion of atoms.[4–10]

The formation of an intermetallic bond layer is a very complex process. In the manufacturing plant, the formed intermetallic bond also may be damaged during the machining process. Specialty ultrasonic instruments are equipped with piston inspection software. Using ultrasonic methods, four process parameters have been recorded:

- travel time of the ultrasonic pulse through the testing device;
- velocity of waves;
- frequency content; and
- relative energy.

The ultrasonic inspection test is usually performed in liquid because sound waves are better emitted in a liquid than in any other environment.[4,11] The aim of this paper is to conduct a detailed metallographic analysis of the intermetallic bonding layer that is formed between the austenitic cast iron ring carrier and the aluminum piston.

Experimental Procedure

The tests were performed on the Ø89 mm piston for diesel engine type OM604 with a turbocharger. The mass of the piston casting with a pouring system and feeder was 1,275g (2.8 lbs) (and the mass of the piston cast was 868g (l.91 lbs). Figure 1 shows a 3D model of the casting and Figure 1b shows the macrostructure at the cross-section of the investigated piston casting. Figure 1c shows an Al-Fin bond with a magnification of 50x and Fig. 1d shows an SEM analysis of the Al-Fin bond with a magnification of 1000x.

The piston alloy composition in Table 1 is close to the eutectic composition and was used to analyze the formation of the Al-Fin bond with a ring carrier. An austenitic cast iron (Ni-Resist) was used to produce the ring carrier (Table 2). The chemical compositions of the ring carriers used herein were in accordance to specifications used by manufacturers.

Table 1. Experimental Alloy Nominal Chemical Composition

Alloy	Chemical composition (wt.%)										
	Si	Cu	Ni	Mg	Fe	Mn	Cr	Ti	Zr	V	Al
AlSi13Cu4Ni2Mg	13.05	3.80	2.01	0.90	0.52	0.19	0.09	0.07	≈0.03	≈0.01	residual

Table 2. Ring Carrier Chemical Composition (wt. %)

	Ni	Cu	C	Cr	Si	Mn	S	P	Fe
Sample	15.10	6.32	2.81	2.21	1.89	1.23	-	-	residual
Standard	13.5–17.5	5.5–7.5	1.0–3.0	0.8–1.2	–	0.5–1.5	>0.1	>0.2	residual

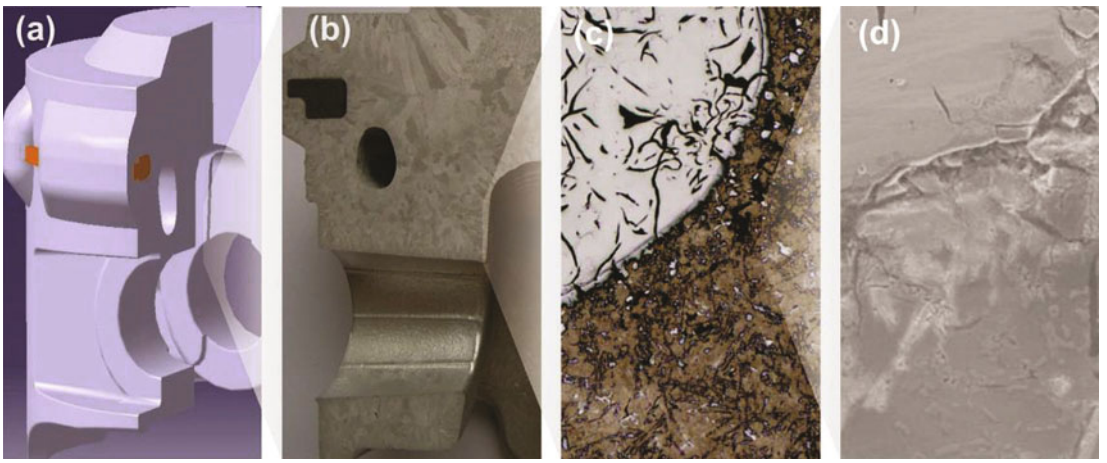

Figure 1. Four different views of the test sample: a) the 3D model of the casting, b) Macrostructure, c) Al-Fin bond, 50x and d) Al-Fin bond, SEM 1000x.

The hardness of the ring carrier in this case was 140–150 HBS (Standard hardness = 120–160 HBS).[5]

Melting was performed in a tub-like electro-resistant inclined furnace, type RIO 750, with power of 80 kW and capacity of 120 kg/h. Preparation of the Al-alloy was performed in electro-resistant muffle furnace with black lead muffle, type RIO 250 and power of 85 kW. In order to improve the mechanical properties of cast pistons, the melt was exposed to the following treatments: refining, modification and degasification. All three operations were performed at 725 ±5°C (1337 ± 9°F). The temperature of the melt was measured using a Ni–Cr–Ni digital pyrometer. In this case, a sodium-based salt was used for refining. The salt is based on sodium and potassium chloride, with a small percentage of cryolite. Modification of the liquid alloy was achieved by gradual dissolution of the prealloy AlTi5B1 in the form of 8mm (0.3 in.) rods.

The rod top was plunged into the liquid Al alloy. This prealloy contained 5% Ti, with ~2.2% of TiB_2, while the remaining 2.8% was Al_3Ti. For improving the mechanical properties of the alloy (i.e., providing a fine grain structure that enables optimal mechanical properties of the cast) 160 ppm of strontium was added to the liquid alloy. Degasification of the Al alloy during these experiments was performed by bleeding it with a mixture of nitrogen and Freon. The casting of test pistons was performed on a semi-automatic machine (the ring carrier was inserted manually). The machine has an automatic cycle operation. Casting machines tilt by 25 to 0 degrees during casting (in this case the tilting started after 5 sec).

In Figure 2 there are four different views of the ring carrier casting: the as-cast surface (Fig. 2a), machined surface (Fig. 2b), the ring carrier was then ultrasonically degreased and held at 750 ± 5°C (1382 ± 9°F) for 6.5 minutes. Then, the ring carrier was inserted into the mold using a specially designed gripper in the mold (Fig. 2c). The piston mold temperature was 245-275°C (473-527°F). The molten Al–Si alloy was poured into the mold over the ring carrier. The ring carrier was observed to embed with the Al alloy after solidification. Next the piston was subjected to machining to create the final shape (Fig. 2d). Sample micrographs were acquired using an Olympus DP70 color digital camera (12.5 megapixel resolution). The samples were observed under a SEM using magnifications between 200x and 5,000x.

Qualitative and quantitative assessments of the chemical compositions of the phases were done using an energy dispersive spectrometer (EDS). A 3D visualization of the alfin layer was made using an OLS4100 laser scanning digital microscope. Thanks to its dedicated objectives with high numerical apertures and a dedicated optical system that obtains superior performance from a laser, it can reliably measure acute-angled samples that were previously impossible to measure. These capabilities also enable measurement of micro-roughness on an uneven surface.

Results and Discussion

The Al-Fin bonding process begins with the growth of an Al alloy intermetallic surface layer on the ring carrier by the immersion of the ring carrier into a molten Al alloy bath.[4,5] The immersion time is determined according to the required layer thickness specification. The ring carrier was uniformly coated with a thin liquid layer (70–100 µm thick) and pulled out of the alloy bath. During a second step, the hot aluminized ring carrier was immediately placed in a preheated metallic mold and a liquid piston alloy was poured into the mold. To obtain a bond at the ring carrier/alloy interface, it was essential at this stage to transfer the insert into the mold and pour the fresh alloy over it at a sufficiently fast rate so that the alloy layer had no time to solidify.

The microstructure of the Al-Fin bond (ring carrier-alfin bond-piston) is shown in Figure 3 at different magnifications (50-500x). In this case, the microstructure of the ring

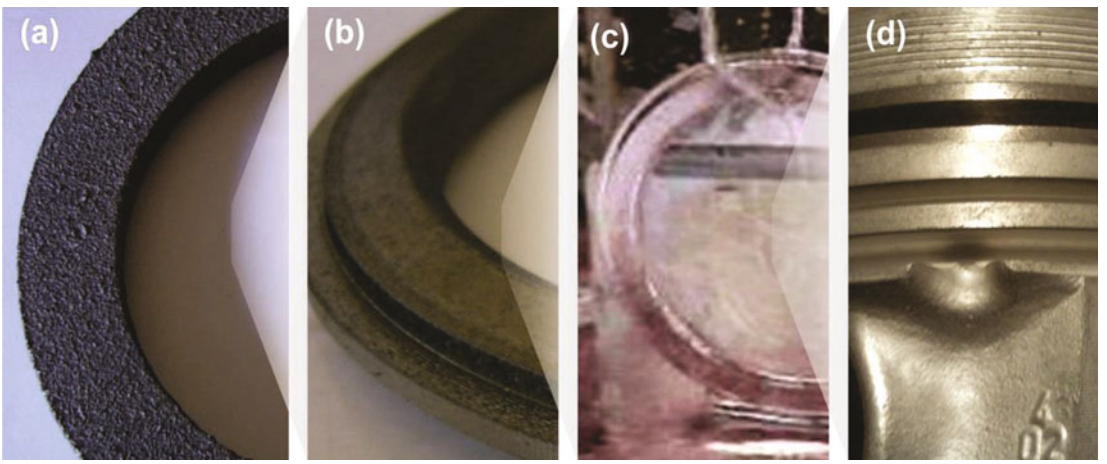

Figure 2. The ring carrier from the casting to the finished part: a) as-cast, b) as machined, c) treaded ring and d) final piston is shown with ring carrier.

carrier consists of lamellar graphite distribution in austenite: ASTM Type A or B, size 4–6. The microstructure of the aluminum piston alloy is also shown in Figure 3. The analyses show that the Al–Si piston alloys have different structures depending on the content of silicon and other alloying elements. Taking into account that the Si crystalized as a primary phase in the eutectic and hypereutectic piston alloys. The solidification sequence could be presented as follows:

$$L\rightarrow(\mathrm{Si}),\ L\rightarrow(\mathrm{Al})+(\mathrm{Si}),\ L\rightarrow(\mathrm{Al})+(\mathrm{Si})+Y \text{ and } L+Y\rightarrow(\mathrm{Al})+(\mathrm{Si})+Y,$$

Where $Y = (Al_3Ni, Al_2Cu, Mg_2Si, Al_3CuNi(Al_3Ni_2), Al_7Cu_4Ni, Al_9FeSi, Al_5FeSi, Al_8FeMg_3Si_6$ and $Al_5Cu_2Mg_8Si_6)$

The primary aluminum phase also appears in the microstructure in hypoeutectic alloys.[1,3,4] Based on the previous studies it has been shown that only these phases may be present in the Al-Si piston alloys, which is the case here as well.

During an experimental procedure, the thickness of the diffusion layer was also measured. The results show that the thickness of the diffusion layer formed in the piston alloy was within the range 18.59 to 48.57 µm (average was 32.39 µm, for an immersion time of 6.5 min). The diffusion layer thickness allowed by international manufacturers of pistons for diesel engines was 10–70 µm.[4]

In order to make a more detailed analysis in addition to characterization by optical and SEM microscopy, a qualitative analysis of the phases in the intermetallic bonding layer was conducted by EDS scanning electron microscopy. In the first step, an EDS mapping of the intermetallic bonding layer was made. In addition to the conventional SEM image, the EDS mapping provides a meaningful picture of the element distribution at the surface. The EDS mapping was done in order to better identify the phases. Additionally, the EDS mapping also provides useful information to predict the possible phases where the key elements show higher contrast. Fig. 4a shows a SEM analysis while Fig. 4b shows an EDS mapping of all elements in the intermetallic bonding layer. The size of the established Al-Fin bond is clearly seen in Fig. 4a and a clear distribution of the alloying elements is seen in Fig. 4b. Figure 4c shows clear distribution of the alloying elements: Al, Si, Fe and Ni. Figures 4d and 4e show the corresponding EDS spectrum for the phase identified in the intermetallic bonding layer. The EDS analysis of the intermetallic bonding layer was conducted in two points. The presence of two intermetallic phases was identified: $FeAl_3$ (Point 1, Fig. 4a) and Fe_2Al_5 (Point 2, Fig. 4a). The EDS results were used to identify the stoichiometry for the particular phases based on the data reported in the literature. The identified phase coincides with the Al-rich phases of the Fe-Al binary phase diagram.[12]

In the second step, a 3D visualization of the intermetallic bonding layer was made. Figure 5a shows the points of line measurement of micro-roughness (Lines 1, 2 and 3) of the intermetallic bonding layer. The results of changes in micro-roughness are shown in Figure 5b, where it is seen in Lines 1 and 2 that there is a height decrease (marked in red), which means that no quality Al-Fin bond was established in this area (in contrast to Line 3). The 3D visualization of the intermetallic bonding layer is shown in Figure 5c, where the points in which no quality Al-Fin bond was established can be easily observed.

Conclusions

Based on the analysis of the experimental tests results presented in this paper, it could be concluded that:

- a good metallic bond can be formed between the two materials of different quality (aluminum piston alloy and austenitic cast iron).
- the thickness of the intermetallic layer (average was 32.39 µm) is small and it is necessary to increase the immersion time (+ 6.5 min).
- the SEM-EDS analysis detected that $FeAl_3$ and Fe_2Al_5 intermetallic phases were formed.
- the visualization and representation of three-dimensional (3D) morphologies of the intermetallic

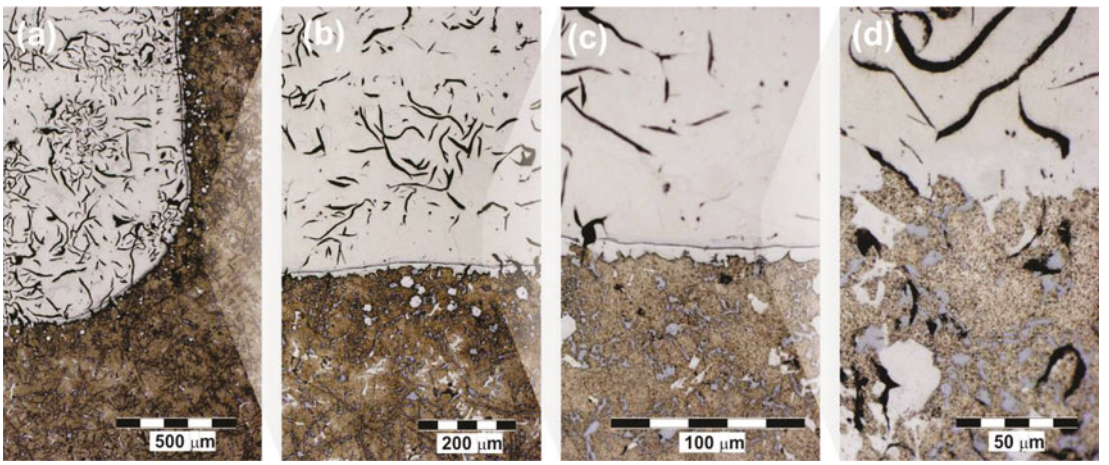

Figure 3. Microstructure of the ring carrier-Al-Fin bond-piston: a)50x, b) 100x, c) 200x and d) 500x.

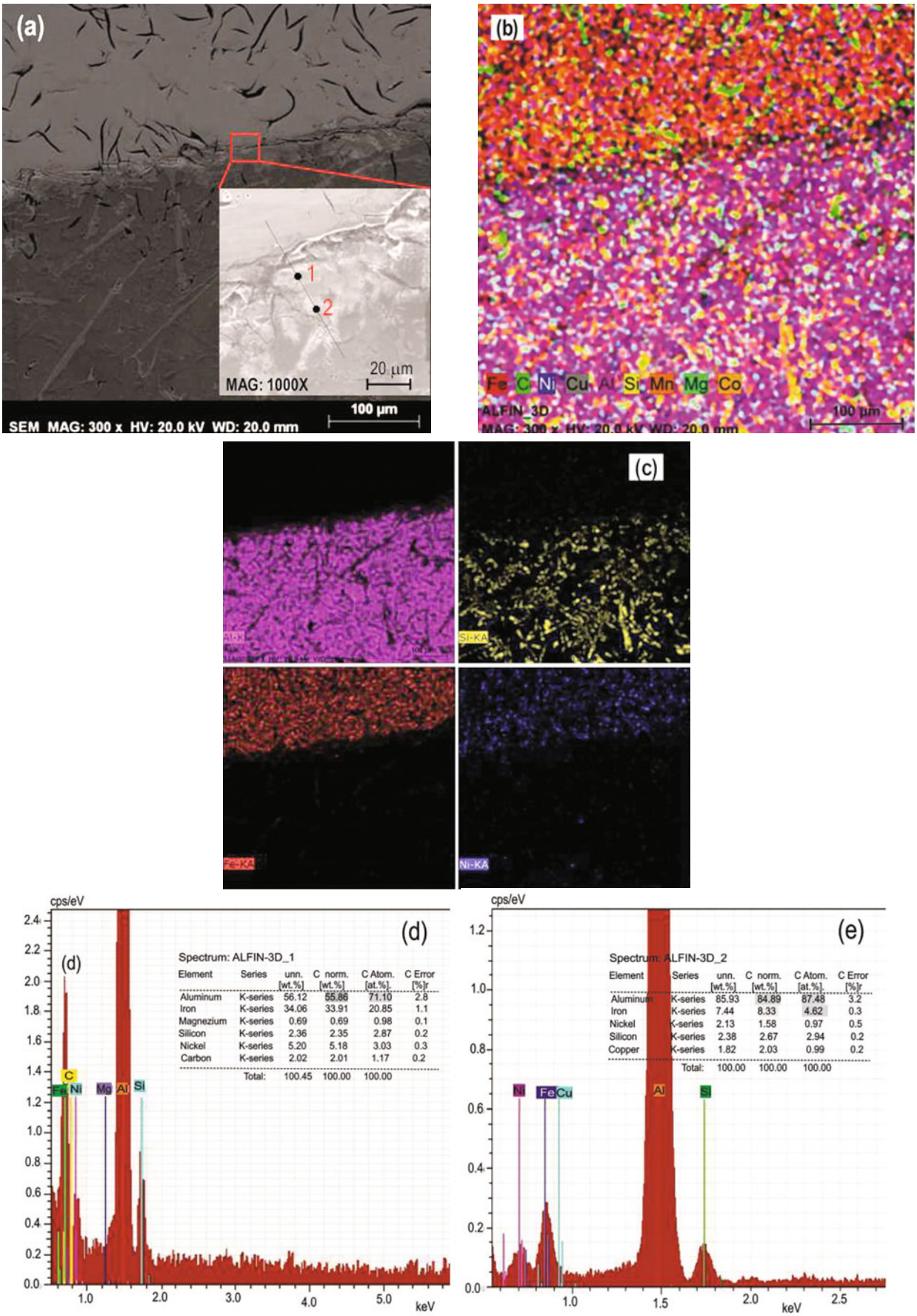

Figure 4. The intermetallic bonding layer: a) SEM, 1000x, b) EDS mapping of all elements, c) EDS mapping Al, Si, Fe and Ni, d) EDS identification of $FeAl_3$ and e) EDS identification of Fe_2Al_5.

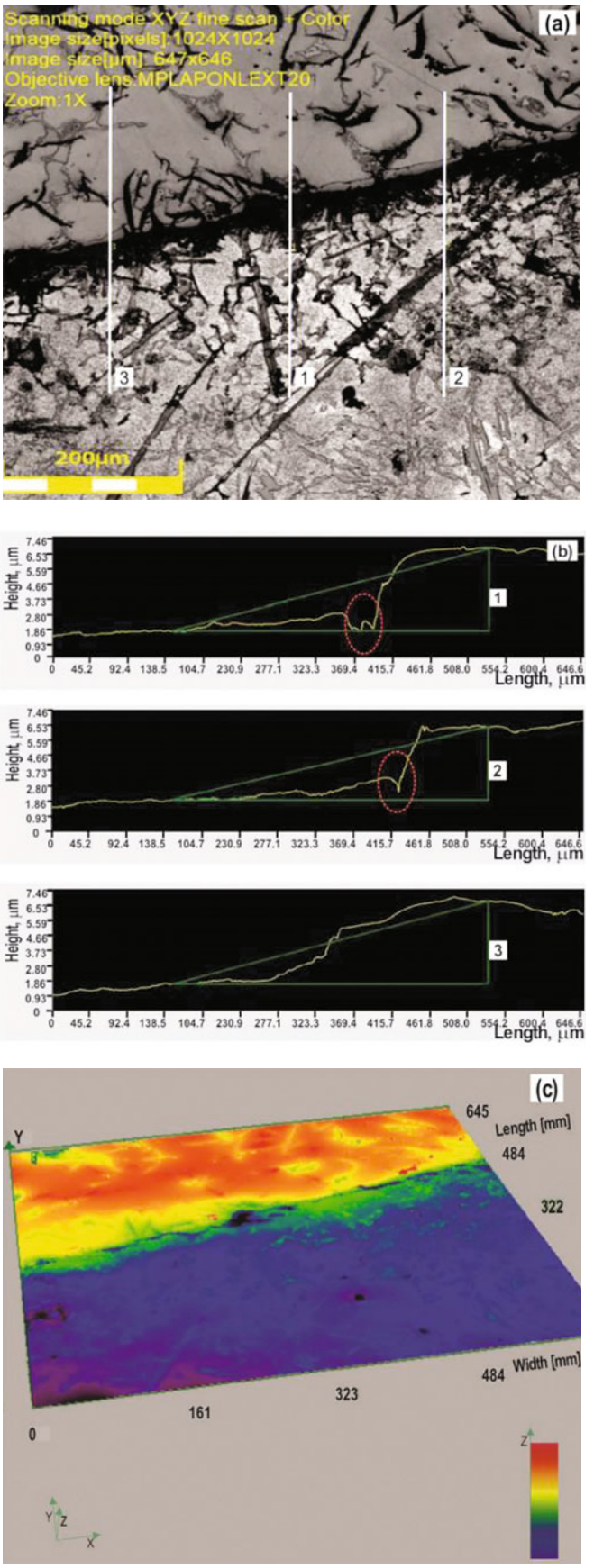

Figure 5. Analysis of the intermetallic bonding layer: a) points marked for line analysis, b) line analysis results and c) 3D visualization

bonding layer are of significant interest for understanding microstructure–properties relationships.

The results presented in this paper are only an introduction to further ongoing research related to the phase composition of the intermetallic bonding layer studied by the XRD analyses and the testing of the mechanical strength of the bond.

Acknowledgements

The research presented in this paper was funded by the Ministry of Education and Science of the Republic of Serbia.

REFERENCES

1. Manasijevic, S., Radisa, R., Markovic, S., Acimovic–Pavlovic, Z., Raic K., "Thermal Analysis and Microscopic Characterization of the Piston Alloy AlSi13Cu4Ni2Mg," *Intermetallics,* vol. 19, pp. 486–492 (2011).
2. Manasijevic, S., Radisa, R., Markovic, S., Raic, K., Acimovic–Pavlovic Z., "Implementation of Infrared Thermography for Thermo-Mechanical Analysis of an AlSi Cast Piston," *Practical Metallography*, vol. 46, pp. 565–579 (2009).
3. Belov, N., Eskin, D., Avxenieva N., "Constituent Phase Diagrams of the Al–Cu–Fe–Mg–Ni–Si System and Their Application to the Analysis of Aluminum Piston Alloys," *Acta Materialia*, vol. 58, pp. 4709–4722 (2005).
4. Manasijevic, S., *Aluminum Piston Alloys*, Published by the LOLA Institute Belgrade (2012).
5. U.S. Patent Number 6,127,046 (Oct. 3, 2000).
6. U.S. Patent Number 6,112,802 (Sep. 5, 2000).
7. Viala, J.C., Peronnet, M., Barbeau, F., Bosselet, F., Bouix, J., "Interface Chemistry in Aluminium Alloy Castings Reinforced with Iron Base Inserts," *Composites: Part A,* vol. 33, pp. 1417–1420 (2002).
8. Uthayakumar, M., Parabhaharan, G., Aravinddan S., Sivaprasad, J.V., "Machining of Bimetallic Piston," *Proceedings of International Conference, ICMAT-2007*, Banerjee, A.J., Chowdhury, A.K., Sinha, G.P. (eds.), Allied Publishers Pvt Ltd., New Delhi, India, pp. 119–124 (2007).
9. Acar, A.F., Ozturk, F., Bayrak, M., "Effects of Variations in Alloy Content and Machining Parameters on the Strength of the Intermetallic Bonding Between a Diesel Piston and a Ring Carrier," *Materials and Technology,* vol. 44, pp. 391–395 (2010).
10. Engine Australia Pty Ltd: *Alfin (Ni-Resist) Ring groove inserts*, Service Engineering Bulletin (2012).
11. Wilcox, M., "Ultrasonic Inspection Equipment for Al-Fin Insert Diesel Pistons," Insight NDT Equipment Ltd., The Old Cider Mill, Kings Thorn, Herefordshire HR2 8AW (2000).
12. Kattner, U.R., *Binary Alloy Phase Diagrams*, T.B. Massalski (ed.), ASM International, Materials Park, OH, pp. 147 (1990).